

# III. Particle interactions with matter

- ❖ All particle detecting techniques are based on interactions of particles with different materials

## Short-range interaction with nuclei

- ❖ Probability of a particle to interact (with a nucleus or another particle) is called *cross-section*.
  - ☉ Cross-sections are normally measured in *millibarns*:  $1 \text{ mb} \equiv 10^{-31} \text{ m}^2$
  - ☉ Total cross-section of a reaction is sum over all possible processes

There are two main kinds of scattering processes:

- ☉ *elastic scattering*: only momenta of incident particles are changed, for example,  $\pi^- p \rightarrow \pi^- p$
- ☉ *inelastic scattering*: final state particles differ from those in initial state, like in  $\pi^- p \rightarrow K^0 \Lambda$

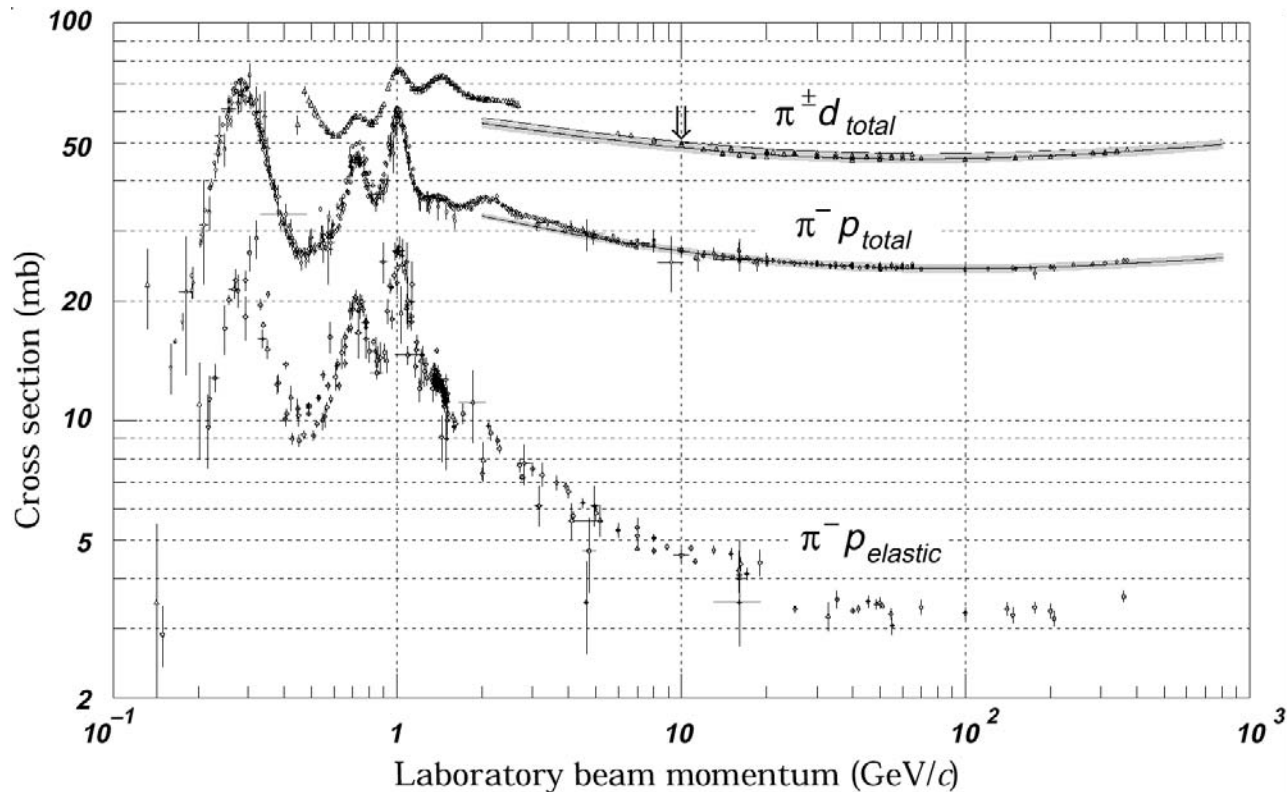


Figure 41: Cross sections of  $\pi^-$  on a fixed proton target

- ⊙ For hadron-hadron scattering, cross-sections are of the same order with the geometrical “cross-sections” of hadrons: assuming their sizes are of order  $r=1\text{ fm} \equiv 10^{-15}\text{ m} \Rightarrow \pi r^2 \approx 30\text{ mb}$
- ⊙ For complex nuclei, cross-sections are bigger, and elastic scattering on a nucleon can cause nuclear excitation or break-up – *quasi-elastic scattering*

Knowing cross-sections and number of nuclei per unit volume in a given material  $n$ , one can introduce two important characteristics:

⊙ *nuclear collision length*: mean path between collisions,  $l_c \equiv 1/n\sigma_{\text{tot}}$

⊙ *nuclear absorption length*: mean path between inelastic collisions,  $l_a \equiv 1/n\sigma_{\text{inel}}$

At high energies, short-range nuclear interactions involve mainly hadrons, facilitating their detection.

Neutrinos and photons have much smaller cross-sections of interactions with nuclei, since former interact only weakly and latter – only electromagnetically.

### *Ionization energy losses*

❖ Energy loss per travelled distance :  $dE/dx$

⊙ Important for all charged particles

⊙ Mostly due to Coulomb scattering of particles off atomic electrons

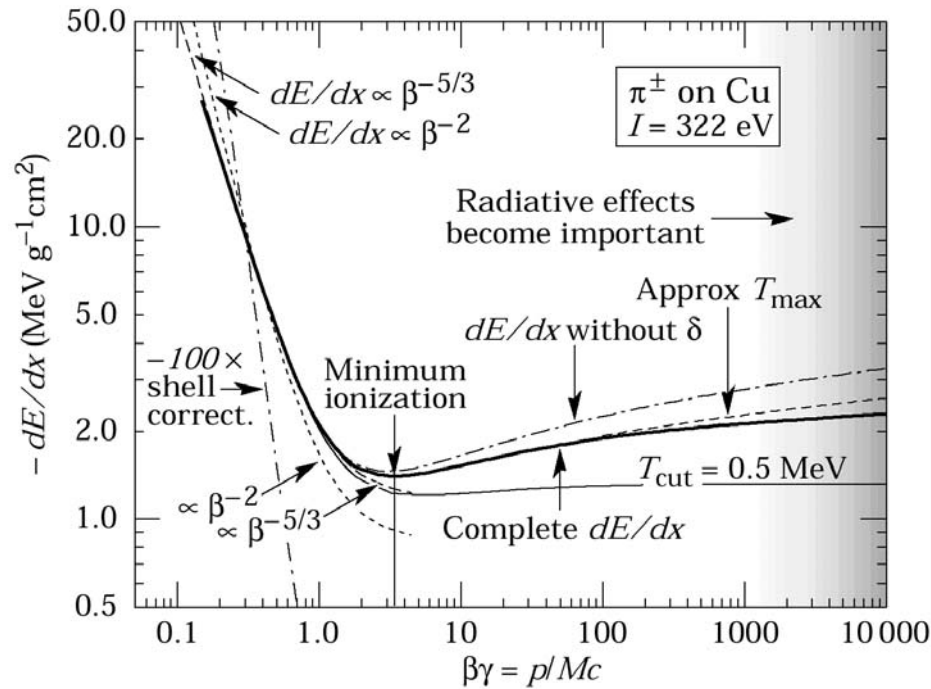


Figure 42: Energy loss rate for pions in copper. At low  $\beta$ ,  $dE/dx$  is proportional to  $1/\beta^2$ . At high  $\beta$ ,  $dE/dx$  proportional to  $\ln(\beta)$

**Bethe-Bloch formula** for spin-0 bosons with charge  $\pm e$  (e.g.  $\pi^+$ ,  $\pi^-$ ,  $K^+$ ,  $K^-$ ):

$$-\frac{dE}{dx} = \frac{Dn_e}{\beta^2} \left[ \ln \left( \left( \frac{2mc^2 \beta^2 \gamma^2}{I} \right) - \beta^2 - \frac{\delta(\gamma)}{2} \right) \right] \quad (31)$$

$$D = \frac{4\pi\alpha^2 \hbar^2}{m} = 5.1 \times 10^{-25} \text{ MeV cm}^2$$

In Equation (34),  $\beta=v/c$  is velocity ( $p=mv$ );  $n_e$ ,  $I$  and  $\delta(\gamma)$  are constants which are characteristic to the medium:

- ⊙  $n_e$  is the electron density,  $n_e = \rho N_A Z / \tilde{A}$ , where  $\rho$  is the mass density of the medium and  $\tilde{A}$  is its atomic weight. Hence, energy loss is strongly *proportional to the density* of the medium
- ⊙  $I$  is the mean ionization potential,  $I \approx 10Z \text{ eV}$  for  $Z > 20$
- ⊙  $\delta(\gamma)$  is a dielectric screening correction, important only for very energetic particles.

### Radiation energy losses

- ❖ Electric field of a nucleus accelerates or decelerates particles, causing them to radiate photons, hence, lose energy: *bremstrahlung* (literally, “braking radiation”)

Bremstrahlung is an important source of energy loss for light particles. It is, however, significant only for high-energy electrons and positrons.

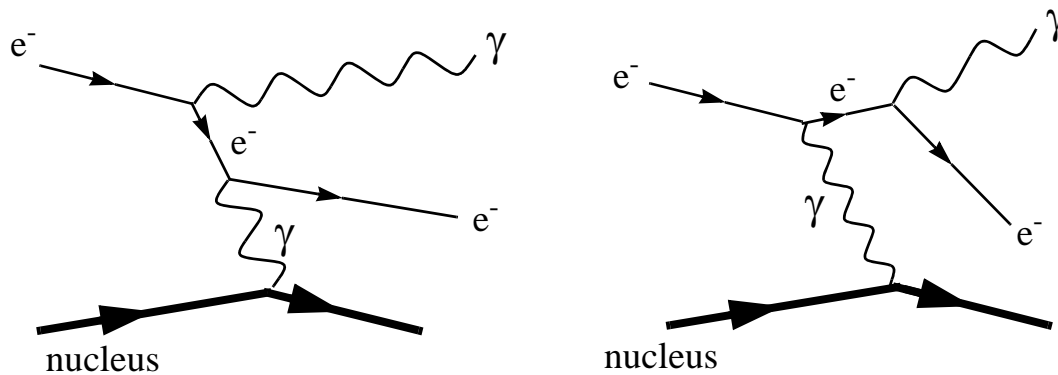


Figure 43: Dominant Feynman diagrams for a bremsstrahlung process  
 $e^- + (Z,A) \rightarrow e^- + \gamma + (Z,A)$

⊙ Contribution to bremsstrahlung from nucleus field is of order  $Z^2\alpha^3$ , and from atomic electrons – of order  $Z\alpha^3$  ( $\alpha^3$  from each electron).

⊙ For relativistic electrons, average rate of bremsstrahlung energy loss is given by:

$$-\frac{dE}{dx} = \frac{E}{L_R} \quad (32)$$

The constant  $L_R$  is called the **radiation length**:

$$\frac{1}{L_R} = 4 \left( \frac{\hbar}{mc} \right)^2 Z(Z+1) \alpha^3 n_a \ln \left( \frac{183}{Z^{1/3}} \right) \quad (33)$$

In Equation (33),  $n_a$  is the density of atoms per  $cm^3$  in medium.

- ❖ Radiation length is the average thickness of material which reduces mean energy of a particle (electron or positron) by factor  $e$ .

### Interactions of photons in matter

Main contributing processes to the total cross-section of photon interaction with atom are:

- ☉ Photoelectric effect ( $\sigma_{p.e.}$ )
- ☉ Compton scattering ( $\sigma_{incoh}$ )
- ☉ Pair production in nuclear and electron field ( $\kappa_N$  and  $\kappa_e$ )



Figure 44: Photoelectric effect (left) and Compton scattering (right)

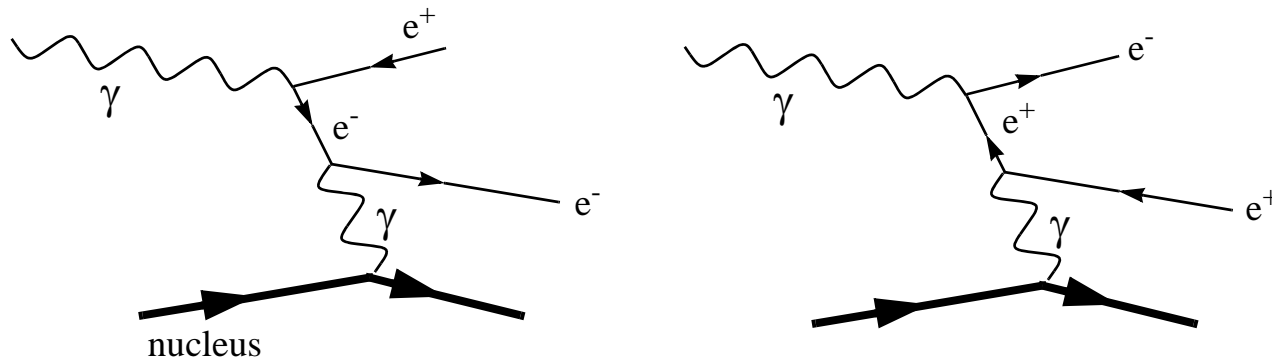


Figure 45: Pair production

At high energies, pair production is the dominant process:  $\sigma_{\text{pair}} = \frac{7}{9} n_a L_R$ , and number of photons travelled distance  $x$  in matter is

$$I(x) = I_0 e^{-7x/9L_R}$$



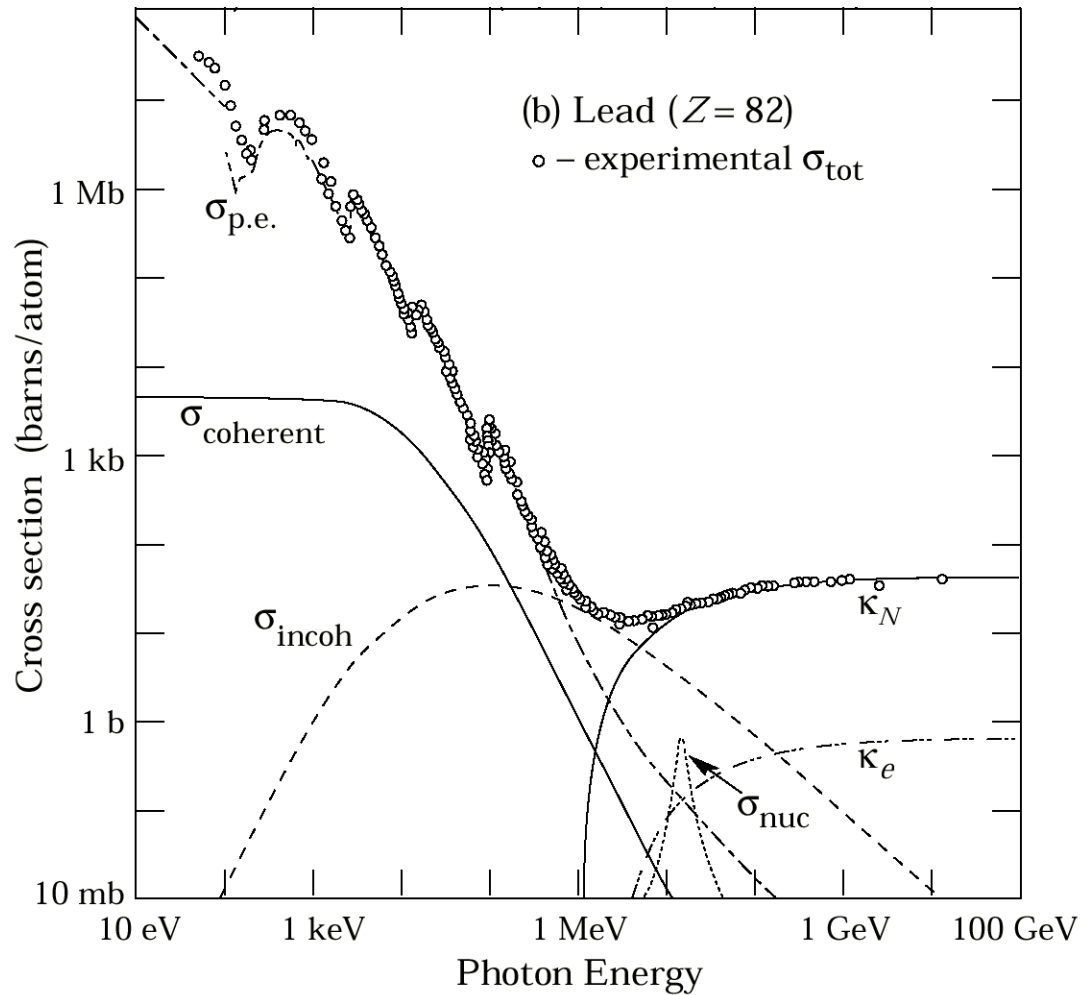


Figure 46: Photon interaction cross-section on a lead atom

☉ Note that pair production occurs when photon energies reach  $E > 2m_e$  ( $E > 1 \text{ MeV}$ ).

# Particle detectors

Particle detectors consist of many subsystems:

- 1) Tracking devices – coordinate measurements
- 2) Calorimeters – energy measurements
- 3) Time resolution counters
- 4) Particle identification devices
- 5) Spectrometers – momentum measurements

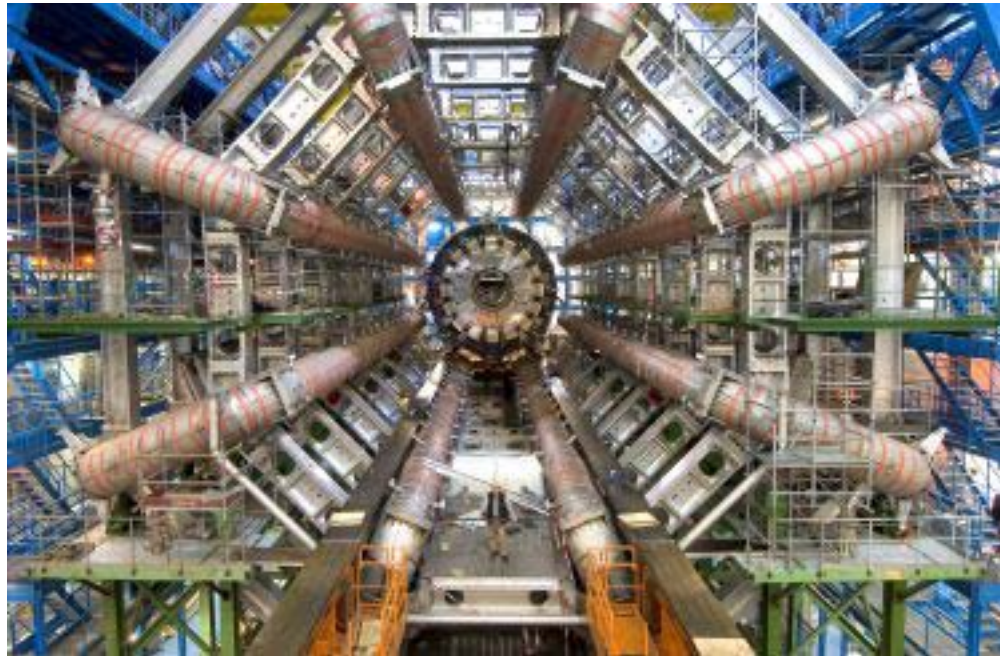


Figure 47: Assembly of the ATLAS detector

## Position measurement

- ❖ Main principle: ionization products are either visualized (as in photoemulsions) or collected on electrodes to produce an electronic signal, to be processed by a computer

Basic requirements of high-energy physics experiments:

- ⊙ High spatial resolution ( $\propto 10\text{-}100\ \mu\text{m}$ )
- ⊙ Possibility to register particles synchronously with a high rate (good *triggering*)

To fulfil the latter, electronic signal pick-up is necessary, therefore photoemulsions and bubble chambers were ultimately abandoned

- ❖ Modern tracking detectors fall in two major categories:
  - ⊙ Gaseous detectors (“*gas chambers*”), resolution  $\sim 100\text{-}500\ \mu\text{m}$
  - ⊙ Semiconductor detectors, resolution  $\sim 5\ \mu\text{m}$

# Proportional and drift chambers

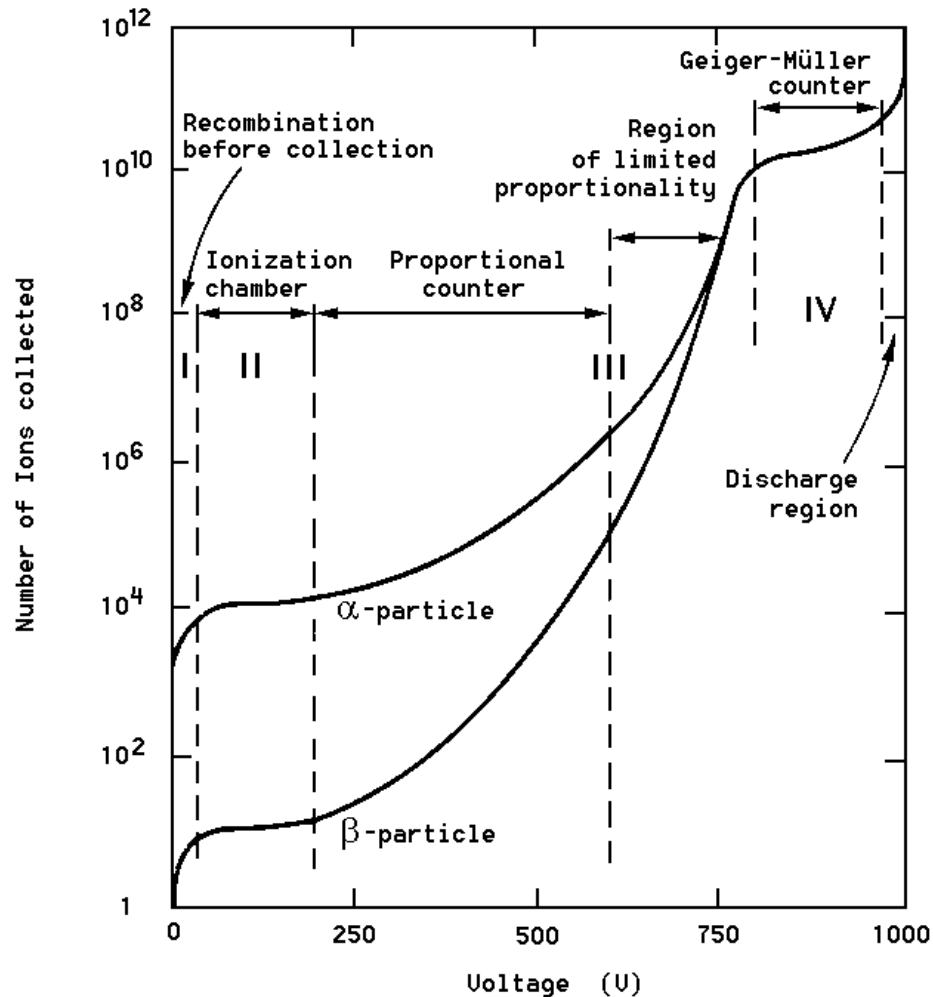


Figure 48: The number of electron-ion pairs collected when a charged particle traverses a gaseous detector of average size, as a function of applied voltage

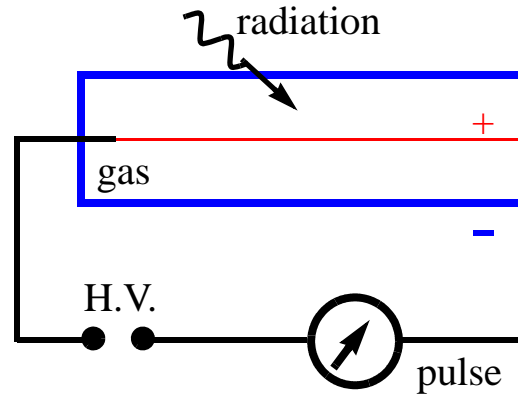


Figure 49: Basic scheme of a wire chamber

### ❖ A simplest proportional chamber:

- A conducting chamber, filled with a gas mixture, serves as a cathode itself, while the wire inside serves as an anode
- The field accelerates the electrons produced in ionization  $\Rightarrow$  secondary electron-ion pairs  $\Rightarrow$  avalanche of electrons  $\Rightarrow$  pulse in the anode. Amplification is  $\propto 10^5$  for voltage of  $10^4$ - $10^5$   $V/cm$ . Gas mixture is adjusted to limit the avalanche.

🎯 Several anode wires  $\Rightarrow$  coordinate measurement possibility (*Multi-Wire Proportional Chamber*, MWPC)

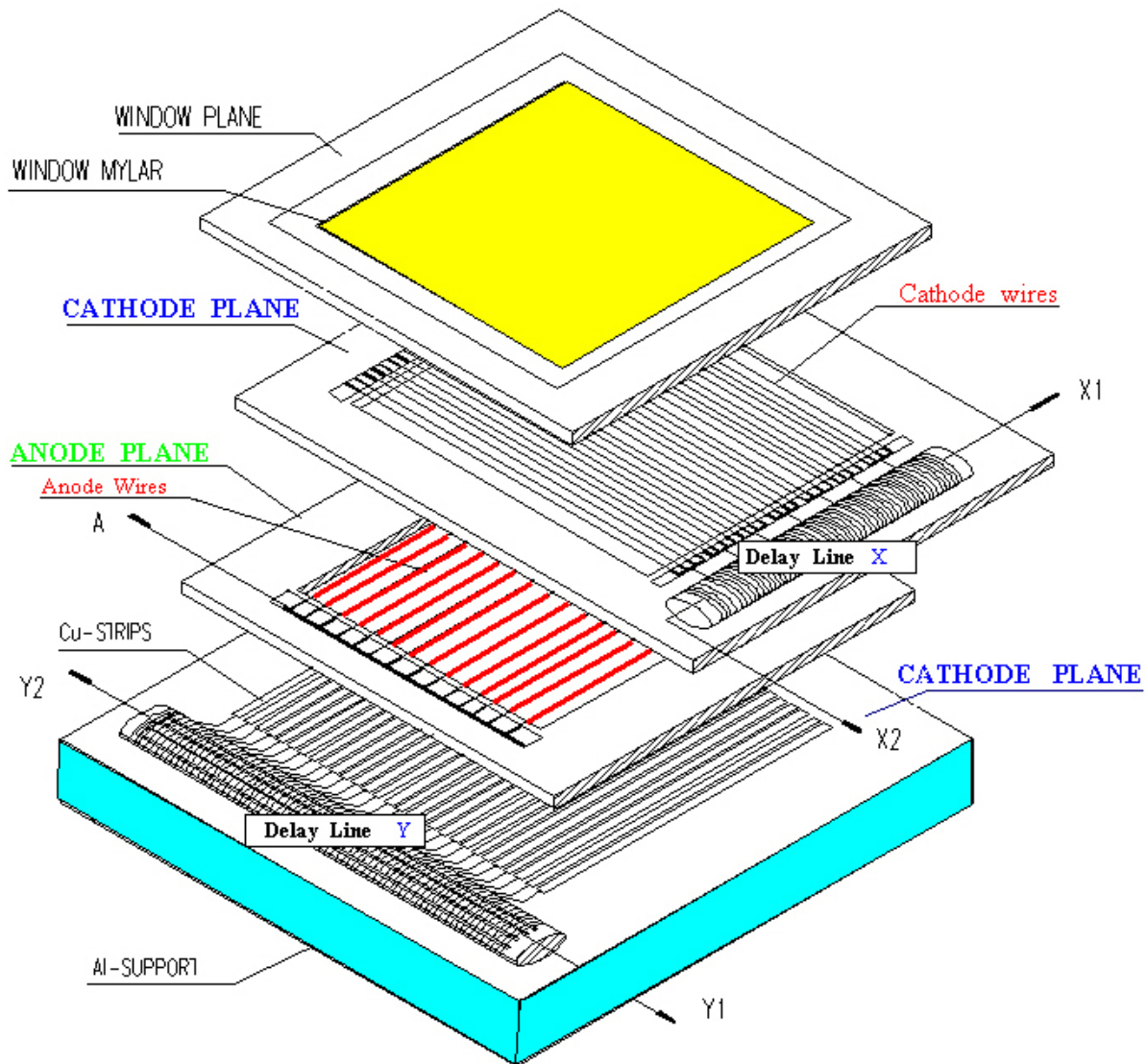


Figure 50: Common view of the 2-dimensional MWPC

## ❖ Alternative to MWPC : *drift chambers*

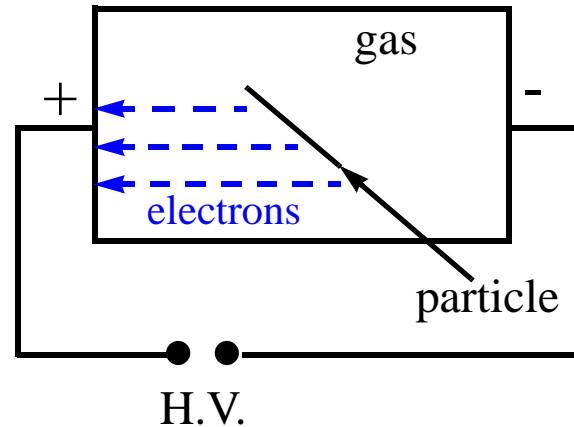


Figure 51: Basic scheme of a drift chamber

- Ionization electrons produced along the particle passage arrive to the pick-up anode at different times  $t_1, t_2, t_3, \dots$
- knowing (from other detectors) the time of particle's arrival  $t_0$  and field in the chamber, one can calculate coordinates of the track  $l_1, l_2, l_3, \dots$
- ⊙ *Streamer detectors* are wire chambers in which secondary ionization is not limited and develops into moving plasmas – *streamers*
- ⊙ If H.V. pulse in a chamber is long enough, a spark will occur: *spark chambers*

# Semiconductor detectors

- ❖ In semiconducting materials, ionizing particles produce electron-hole pair. Number of these pairs is proportional to energy loss by particles

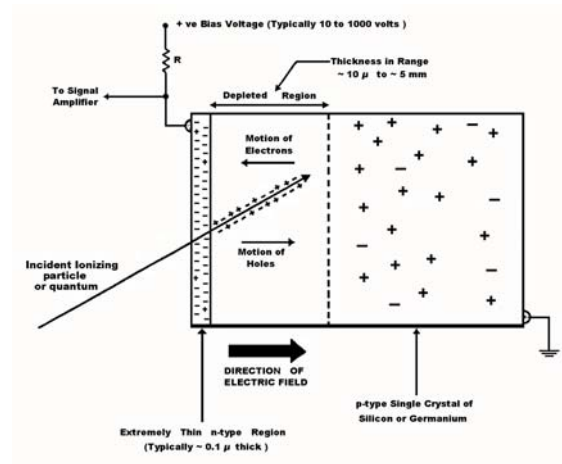


Figure 52: Typical silicon detector is a p-n junction diode operated at reverse bias

- ⊙ Superior resolution (few  $\mu m$ ), small size, small power consumption, fast signals.
- ⊙ Subject to radiation damages; can be circumvented by using radiation-hard manufacturing processes, appropriate handling (e.g. cooling) and by using very thin detectors.



## Calorimeters

- ❖ To measure energy (and position) of the particle, calorimeters use absorbing material to capture all the energy of the particle.
- ❖ Signals produced in calorimeters are proportional to the energy of the incoming particle.
- ❖ During the absorption process, particle interacts with the material of the calorimeter and produces a secondary *shower* of particles.
- ❖ Since *electromagnetic* and *hadronic* showers are somewhat different, there are two corresponding types of calorimeters

# Electromagnetic calorimeters

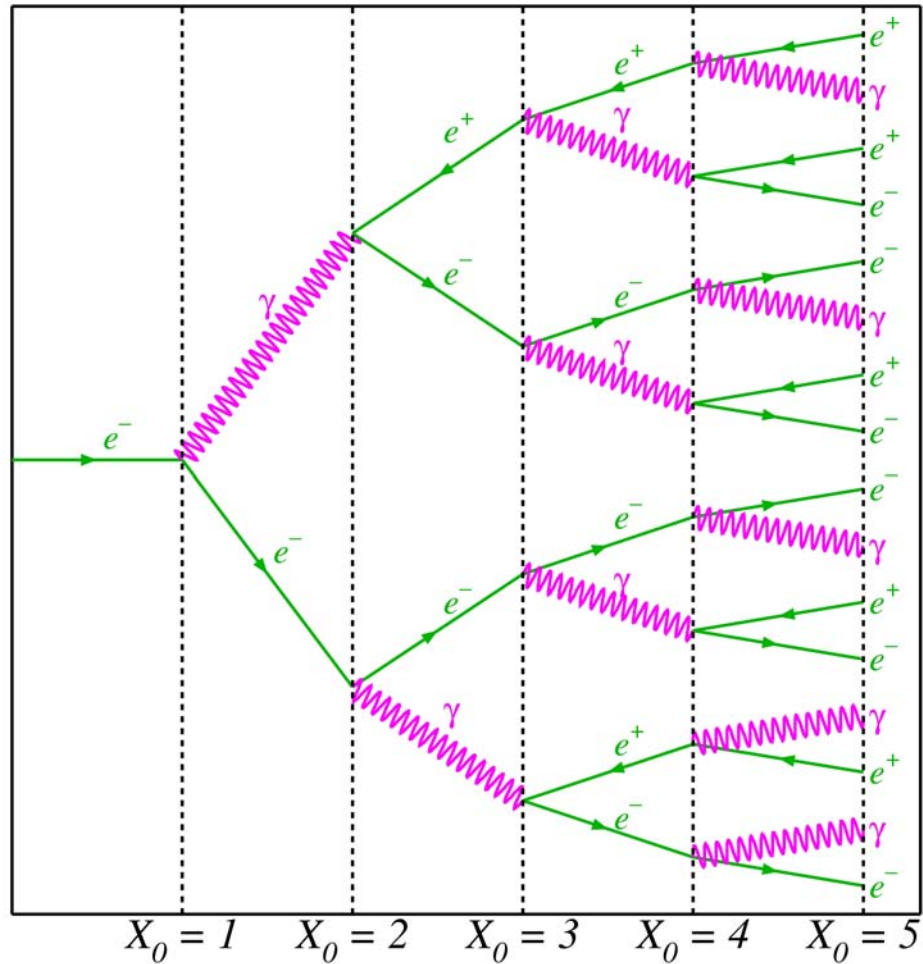


Figure 53: Electromagnetic shower; depth in radiation lengths

## ❖ Used for electron/positron and $\gamma$ energy measurements

- ⊙ Dominant energy loss for high-energy electrons (or positrons) is bremsstrahlung:  
 $e^- \rightarrow e^- \gamma$
- ⊙ Photons produced via bremsstrahlung produce  $e^+e^-$  pairs and are thus absorbed again:  $\gamma \rightarrow e^+e^-$
- ⊙ An initial electron thus produces a cascade of photons and  $e^+e^-$  pairs, until its energy falls under the bremsstrahlung threshold of  $E_C \approx 600 \text{ MeV}/Z$

❖ A calorimeter has to be large enough to absorb all the possible energy of the incoming particle.

## Main assumptions for electromagnetic showers:

- Each electron with  $E > E_C$  travels one radiation length and radiates a photon with  $E_\gamma = E/2$
- Each photon with  $E_\gamma > E_C$  travels one radiation length and creates an  $e^+e^-$  pair, which shares equally  $E_\gamma$
- Electrons with  $E < E_C$  cease to radiate; for  $E > E_C$  ionization losses are negligible

These considerations lead to the expression:

$$t_{max} = \frac{\ln(E_0/E_C)}{\ln 2} \quad (34)$$

where  $t_{max}$  is number of radiation lengths needed to stop the electron of energy  $E_0$ .

Electromagnetic calorimeters can be, for example, lead-glass (crystal) blocks collecting the light emitted by showers, or a drift chamber interlayed with heavy absorber material (lead).

# Hadron calorimeters

- ❖ Used for hadron energy measurement ( $\pi$ ,  $K$ , protons, neutrons)
  - ☉ Hadronic showers are similar to the electromagnetic ones, but absorption length is larger than the radiation length of electromagnetic showers since hadrons interact in the material through nuclear interactions.
  - ☉ Also, some contributions to the total absorption may not lead to a signal in the detector (e.g., nuclear excitations or secondary neutrinos)

Main characteristics of a hadron calorimeter are:

- It has to be thicker than electromagnetic one
  - Layers of  $^{238}\text{U}$  can be introduced to compensate for energy losses (low-energy neutrons cause fission)
  - energy resolution of hadron calorimeters is generally rather poor
- ❖ Hadron calorimeter is usually a set of MWPC's or streamer tubes, interlayed with thick iron absorber

# Scintillation counters

- ❖ Scintillation counters are widely used to detect the passage of charged particles through an experimental setup and to measure particle's "*time-of-flight*" (TOF).
- ❖ Scintillators are materials (crystals or organic) in which ionizing particles produce visible light without losing much of its energy
  - 🌀 The light is guided down to photomultipliers and is being converted to a short electronic pulse.

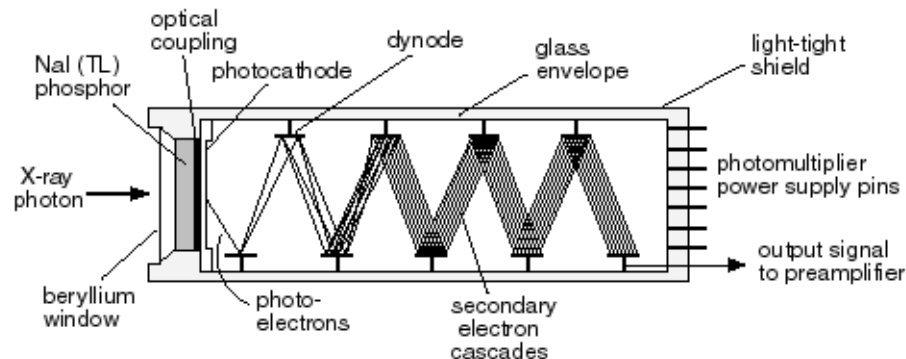


Figure 54: Scheme of a scintillation detector and photomultiplier assembly

## Particle identification

- ⊙ Particles are identified by mass and charge: knowing momentum of particle is not enough to find those out, complementary information is needed.
  - ⊙ For low-energy particles ( $E < 1 \text{ GeV}$ ), TOF counters can provide this complementary data.
  - ⊙ Energy loss rate  $dE/dx$  depends on particle mass for energies below  $\approx 2 \text{ GeV}$  ( $1/\beta^2$  region of Bethe-Bloch formula)
- ❖ The most reliable particle identification device: *Cherenkov counters*
- ⊙ In certain media, energetic charged particles move with velocities higher than the speed of light in these media
  - ⊙ Excited atoms along the path of the particle emit coherent photons at a characteristic angle  $\theta_C$  to the direction of motion

The angle  $\theta_C$  depends on the refractive index of the medium  $n$  and on the particle's velocity  $v$ :

$$\cos\theta_C = c/vn \quad (35)$$

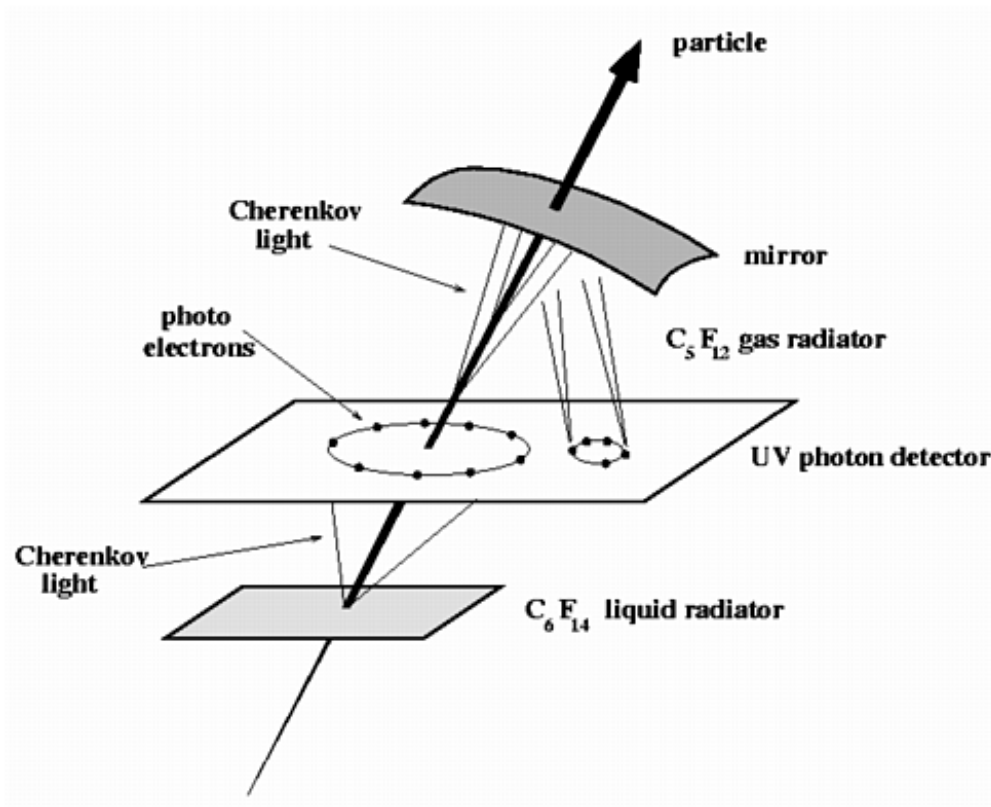


Figure 55: Cherenkov effect in the DELPHI RICH detector

- Measuring  $\theta_C$ , the velocity of the particle can be easily derived, and the identification performed:  $p$  is measured by a tracking device,  $v$  by the Cherenkov counter  $\Rightarrow m=p/v$ .



## Transition radiation measurements

- ⊙ In ultra-high energy region, particles velocities do not differ very much
- ⊙ Whenever a charged particle traverses a border between two media with different dielectric properties, a *transition radiation* occurs
- ⊙ Intensity of emitted radiation is sensitive to the particle's energy  $E = \gamma mc^2$ .
- ⊙ Transition radiation occurs only if  $\gamma > 1000$ , which means  $E/m > 1000$ .

Transition radiation measurements are particularly useful for separating electrons from other particles: for electrons,  $\gamma = 1000$  for  $E = 0.5 \text{ GeV}$ . For pions,  $\gamma = 1000$  for  $E = 135 \text{ GeV} \Rightarrow e/\pi$  separation between 0.5 and 135 GeV.

## Spectrometers

- ❖ Momenta of particles can be measured by curvatures of tracks in a magnetic field:  $p = 0.3B\rho$ , where  $\rho$  is curvature,  $B$  is magnetic field.

*Spectrometers* are tracking detectors placed inside a magnet, providing momentum information

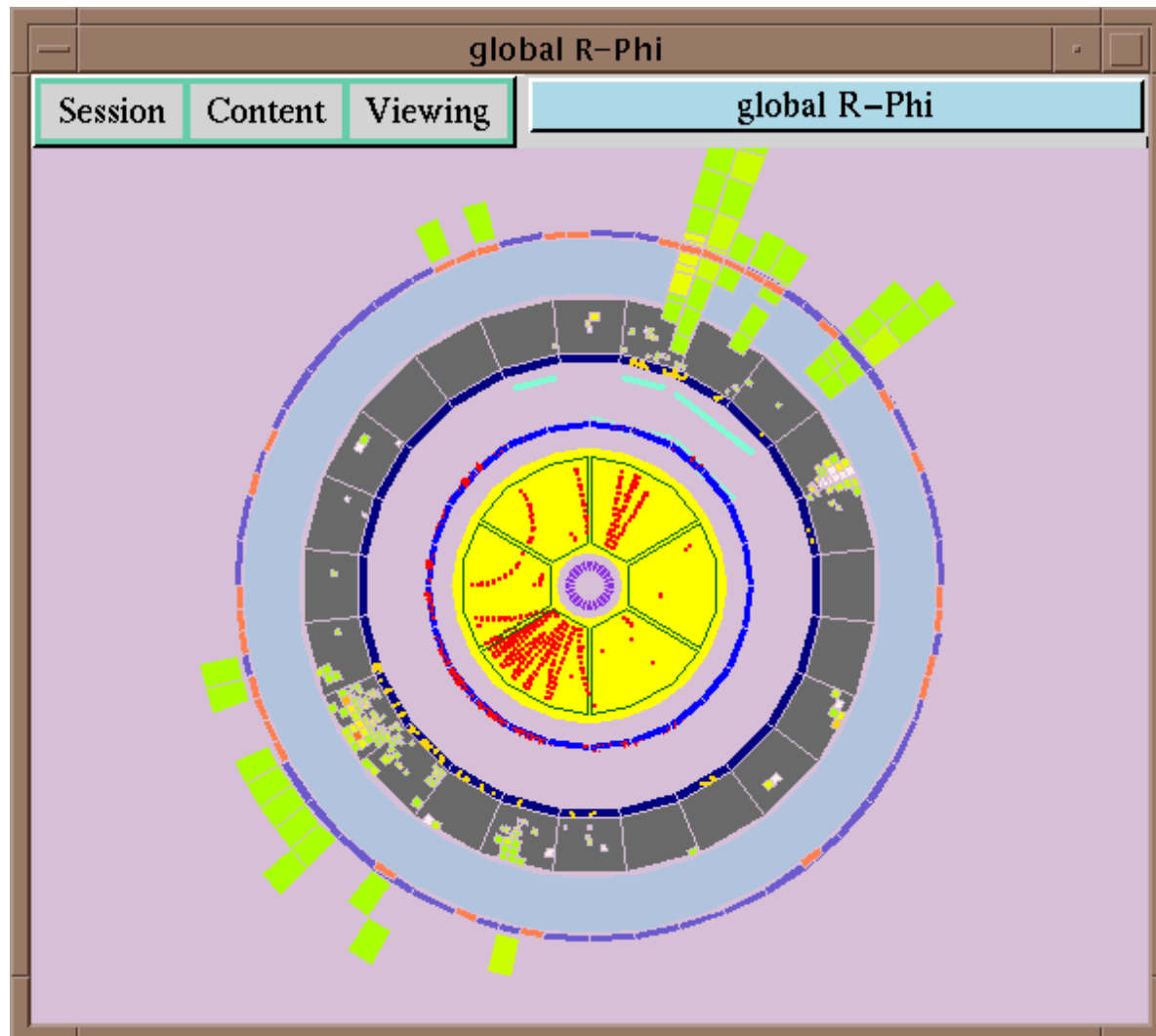


Figure 56: A  $e^+e^-$  annihilation event as seen by the DELPHI detector. In collider experiments, all the tracking setup is typically contained inside a solenoidal magnet.

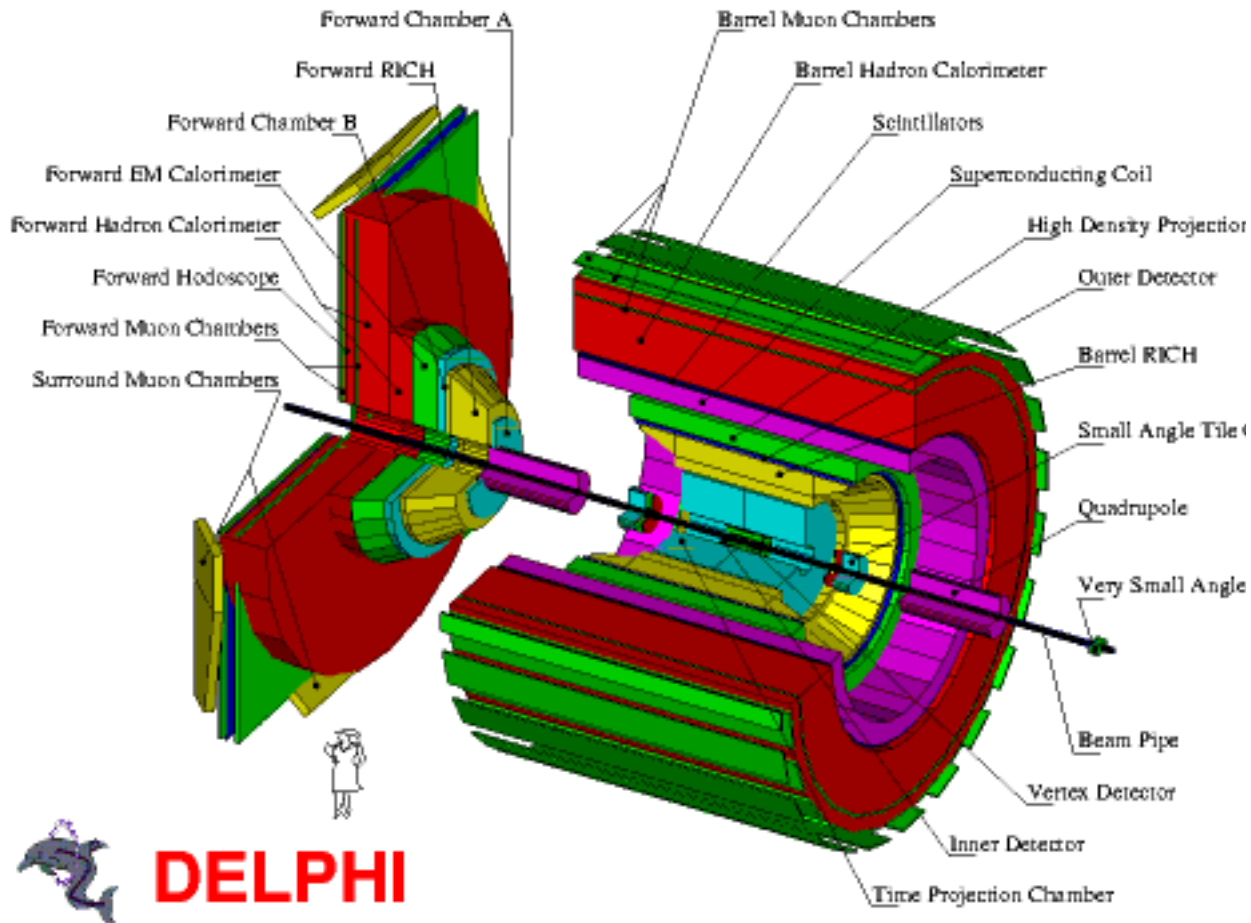


Figure 57: The DELPHI detector at LEP (operated in 1989 - 2001)  
 ~10 meters long, 3500 tons

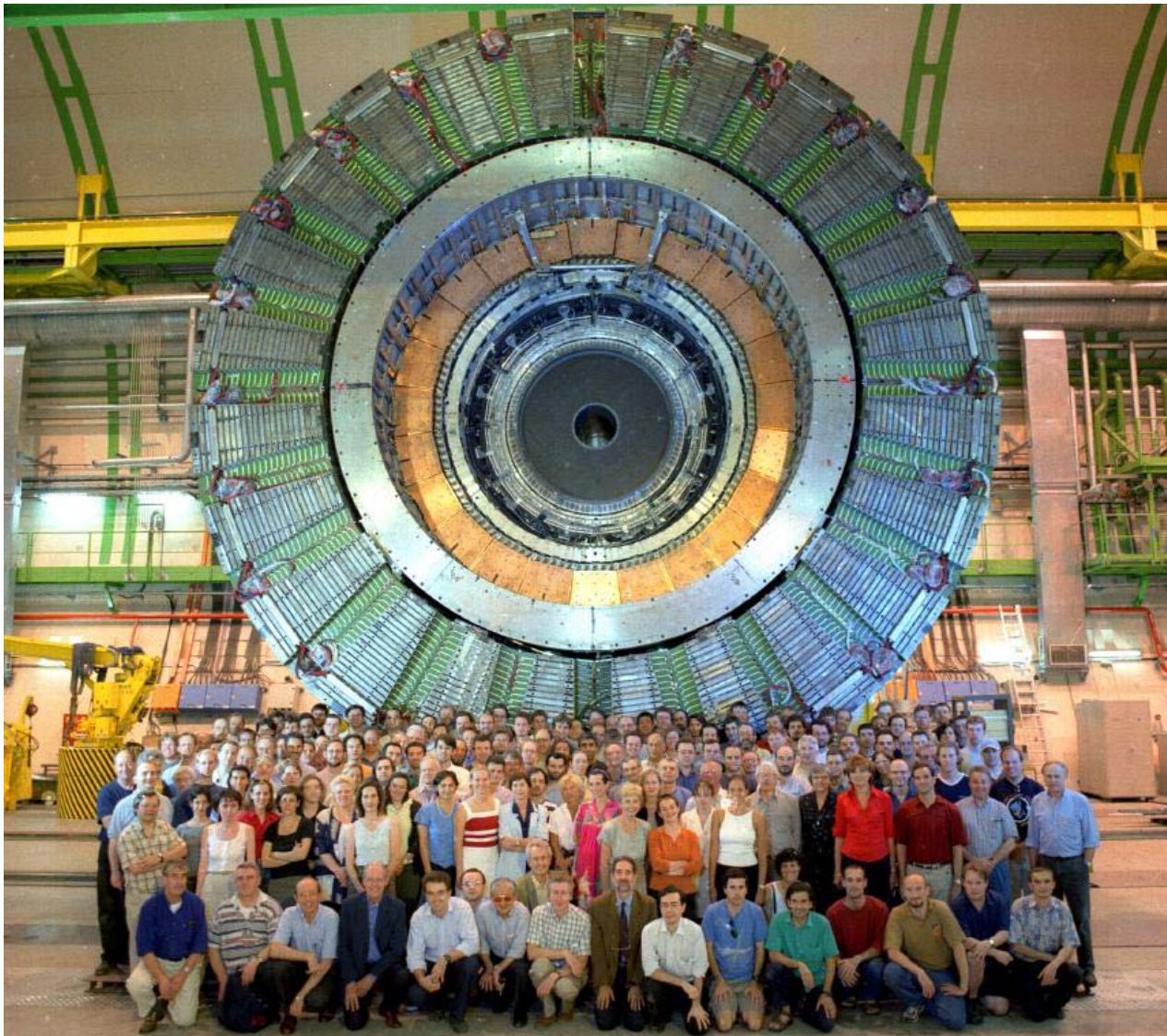


Figure 58: DELPHI detector being disassembled

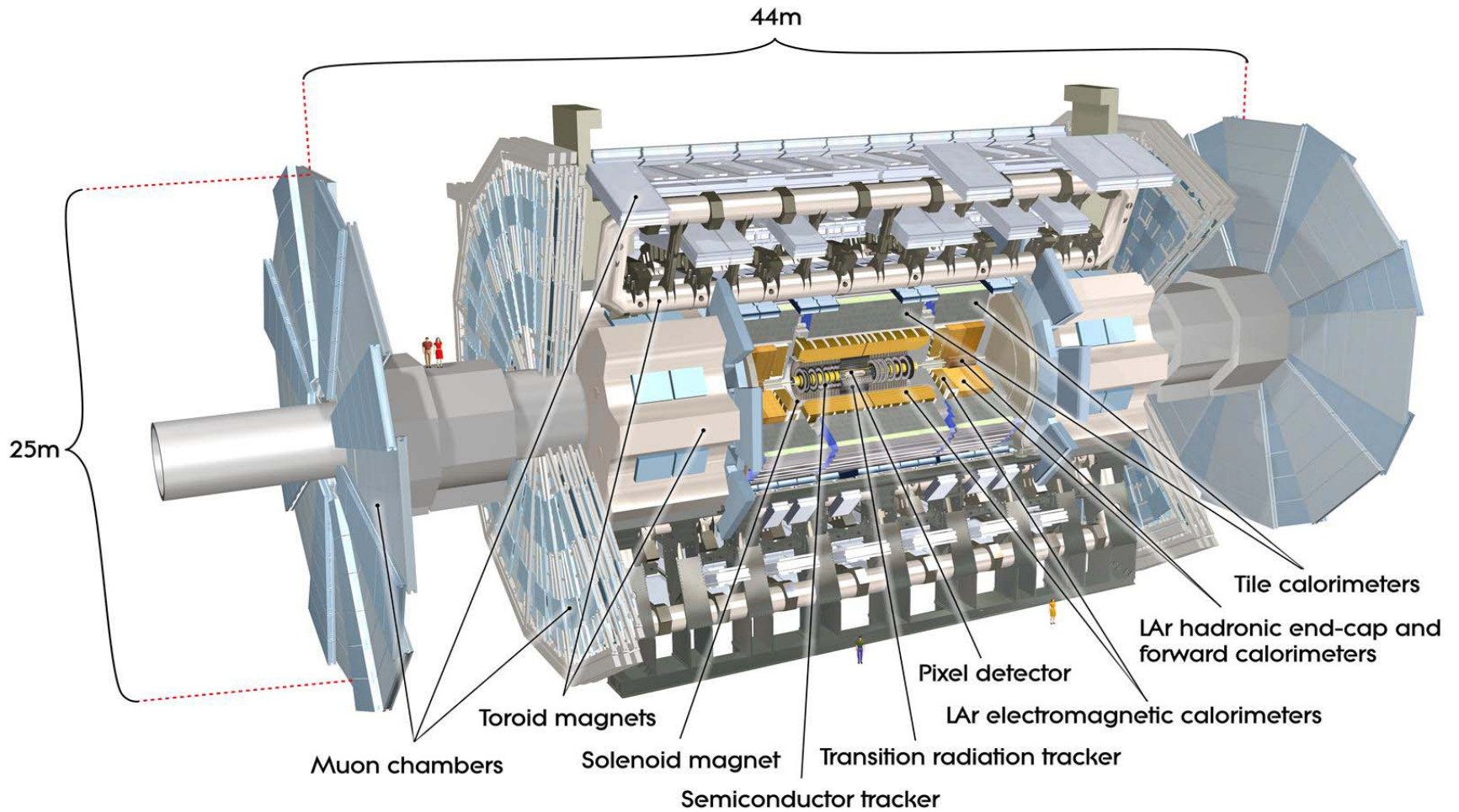


Figure 59: ATLAS detector at LHC, operates since 2008  
44m long, 7000 tons

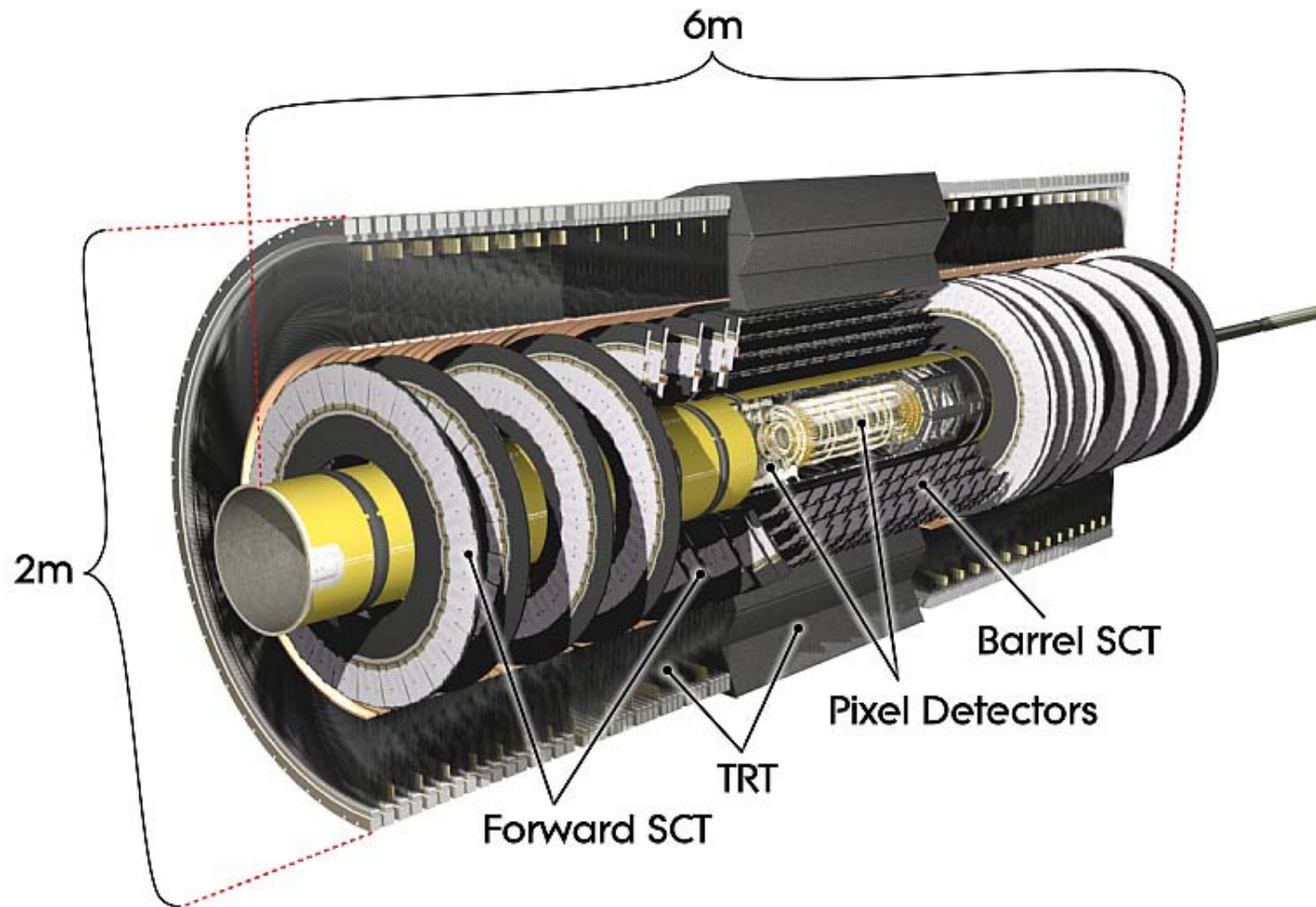


Figure 60: ATLAS Inner Detector: semiconductor trackers and the transition radiation tracker

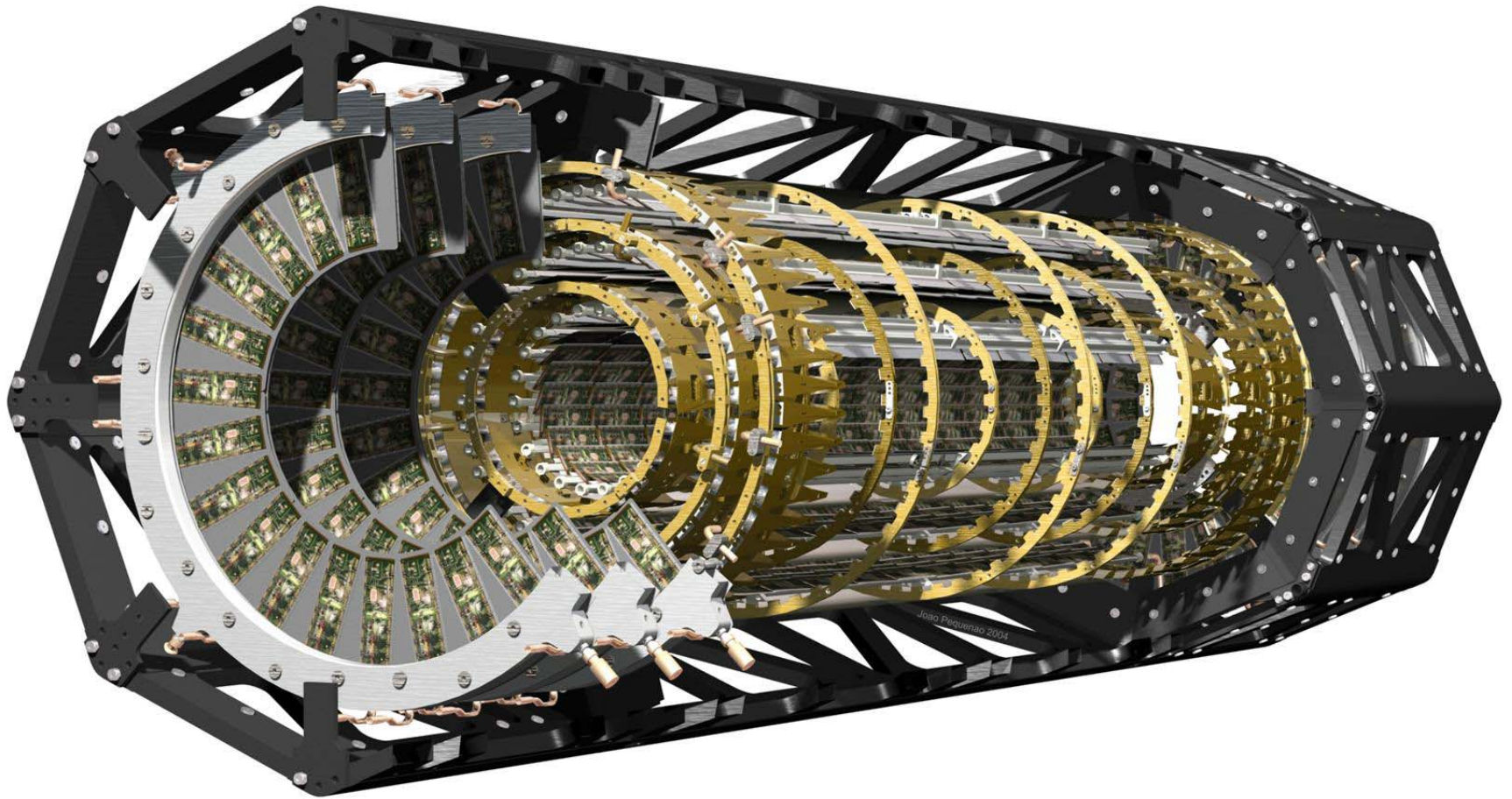


Figure 61: ATLAS Pixel Detector close-up

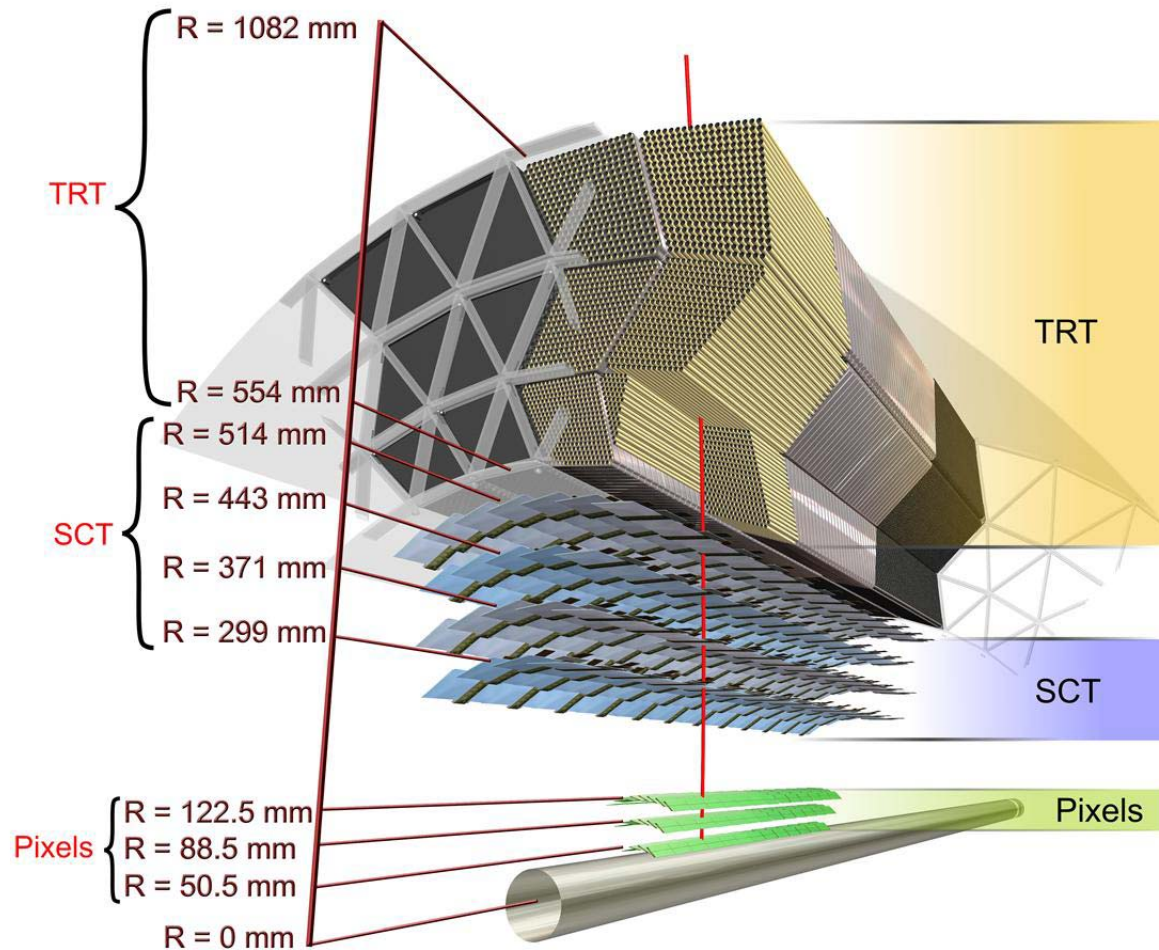


Figure 62: ATLAS inner trackers as seen by a particle



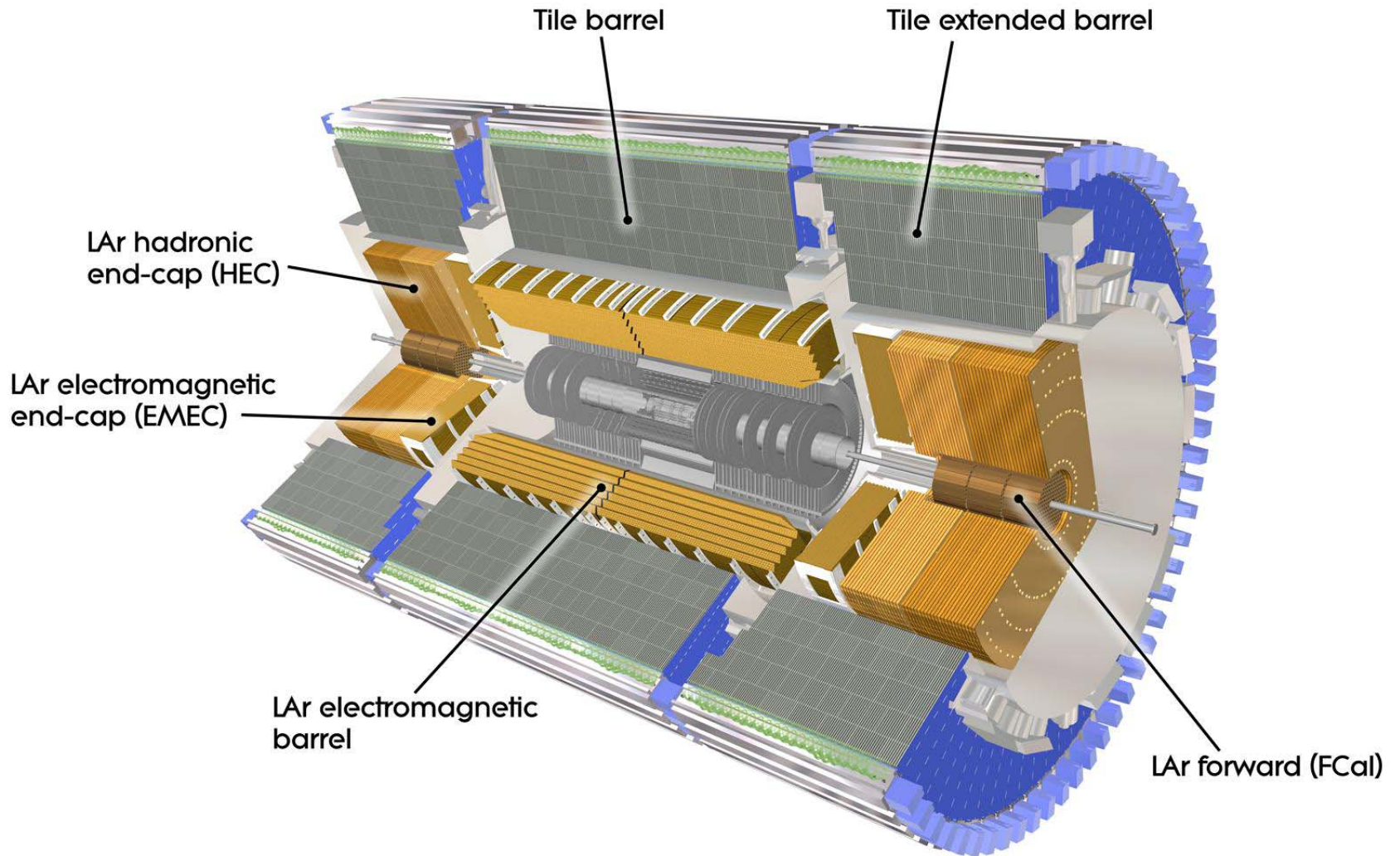


Figure 63: ATLAS calorimeters. LAr (for “liquid Argon”): EM and hadronic (absorbers: lead, copper, tungsten). TileCAL - hadronic, steel/scintillator

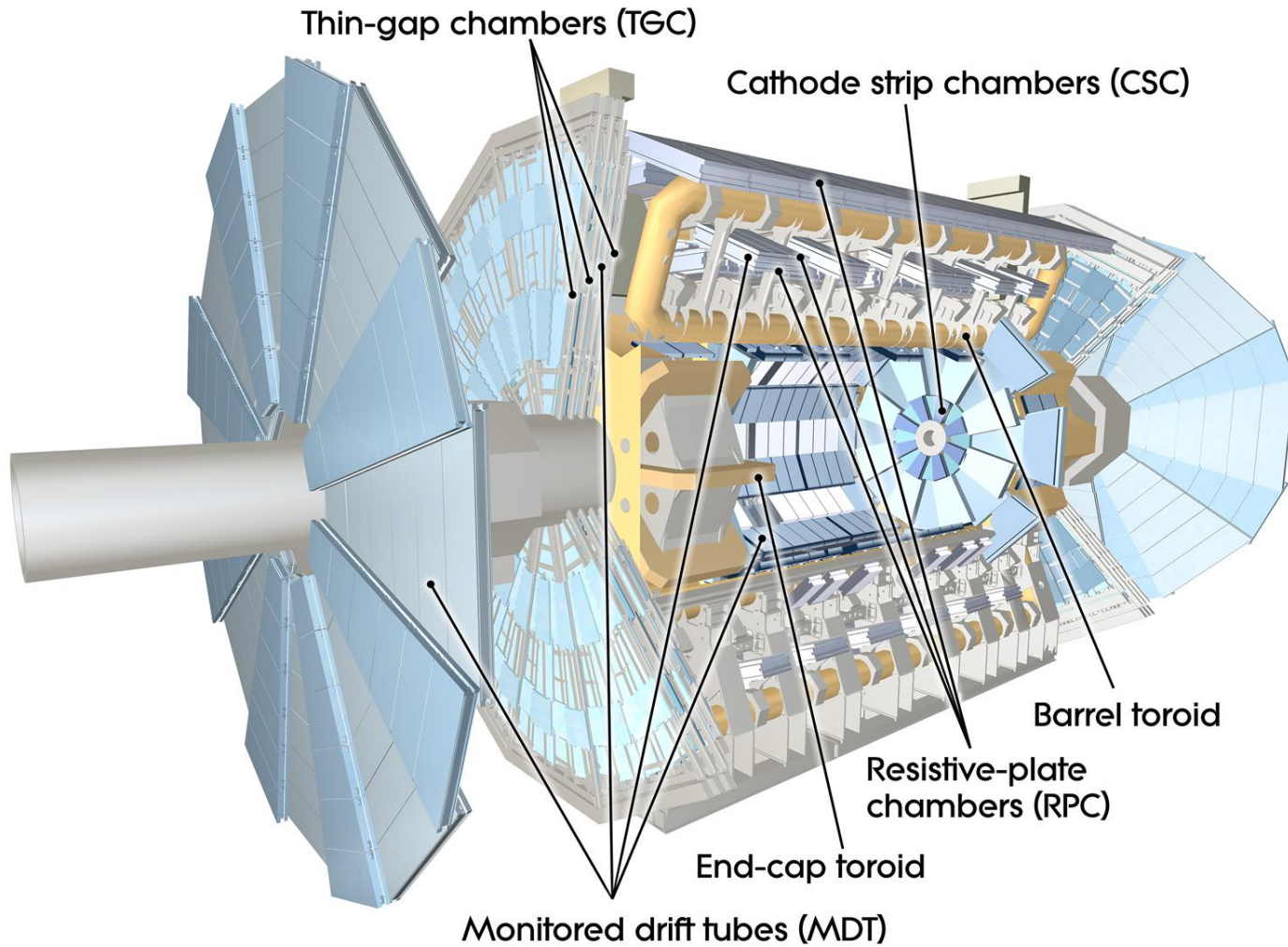


Figure 64: ATLAS muon systems



Figure 65: ATLAS solenoid (left) and end-cap toroid (right)

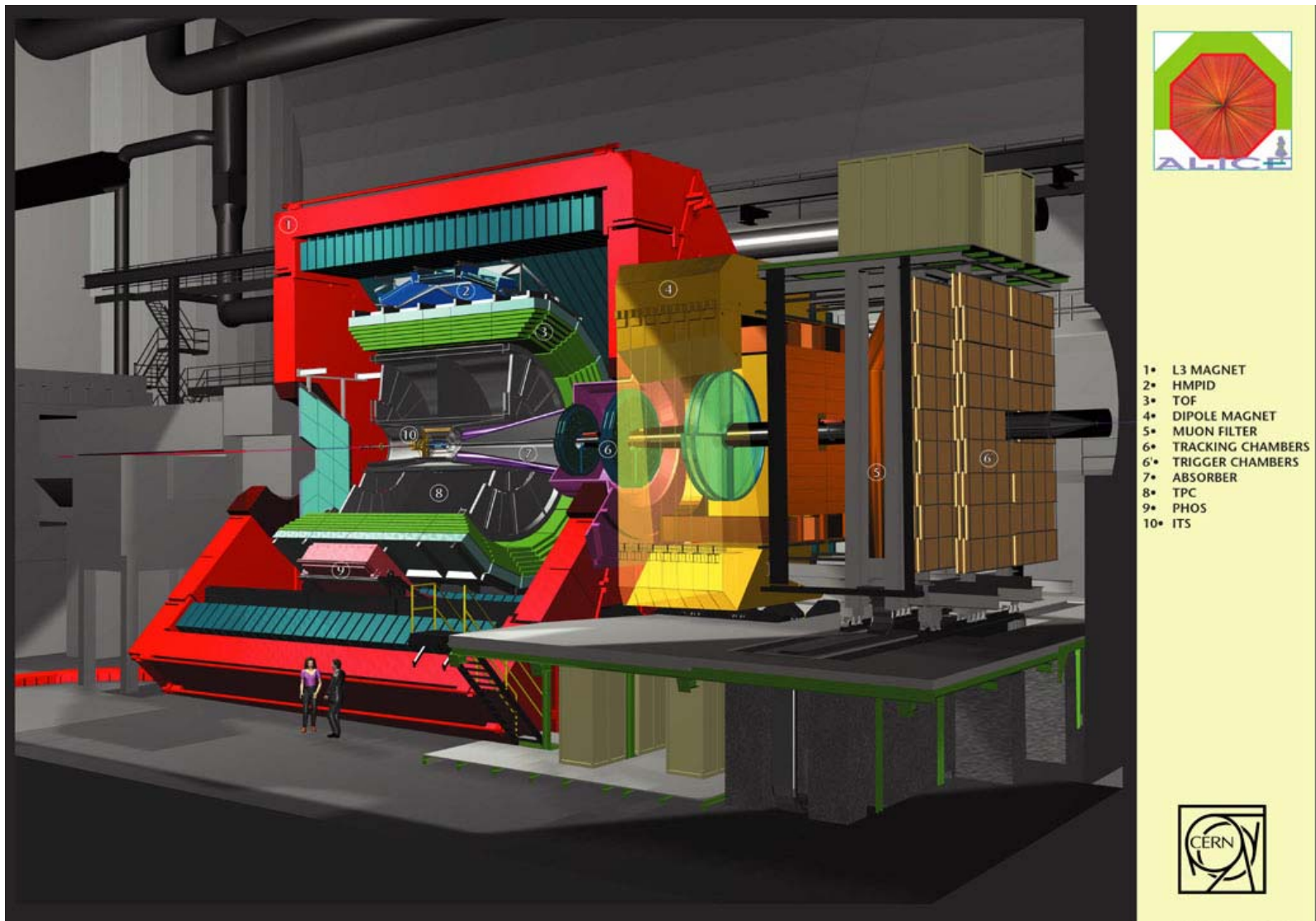


Figure 66: ALICE detector at LHC - dedicated to Pb-Pb collision measurements



# LHC-B Detector

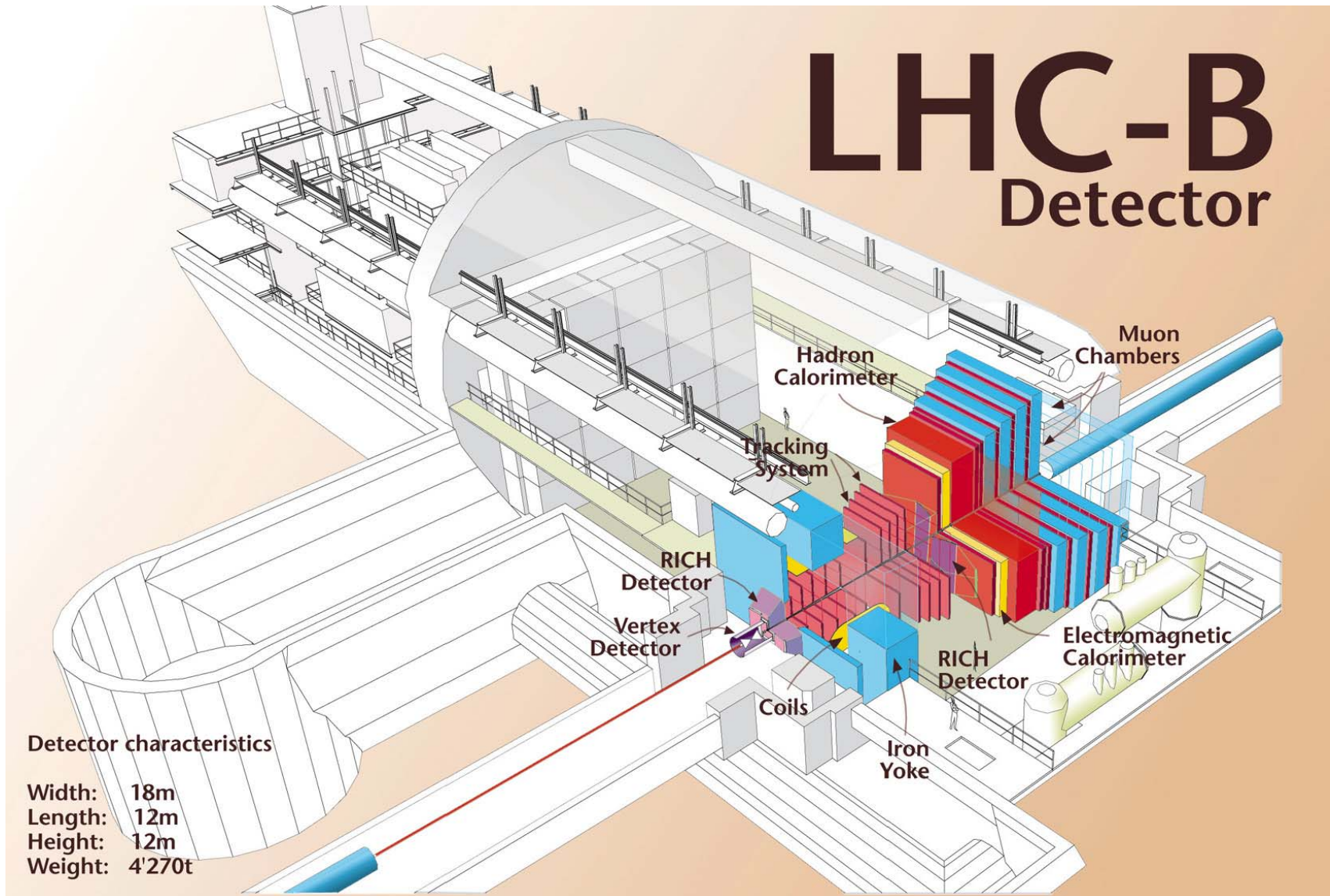


Figure 68: LHC-b detector at LHC, dedicated to B meson studies

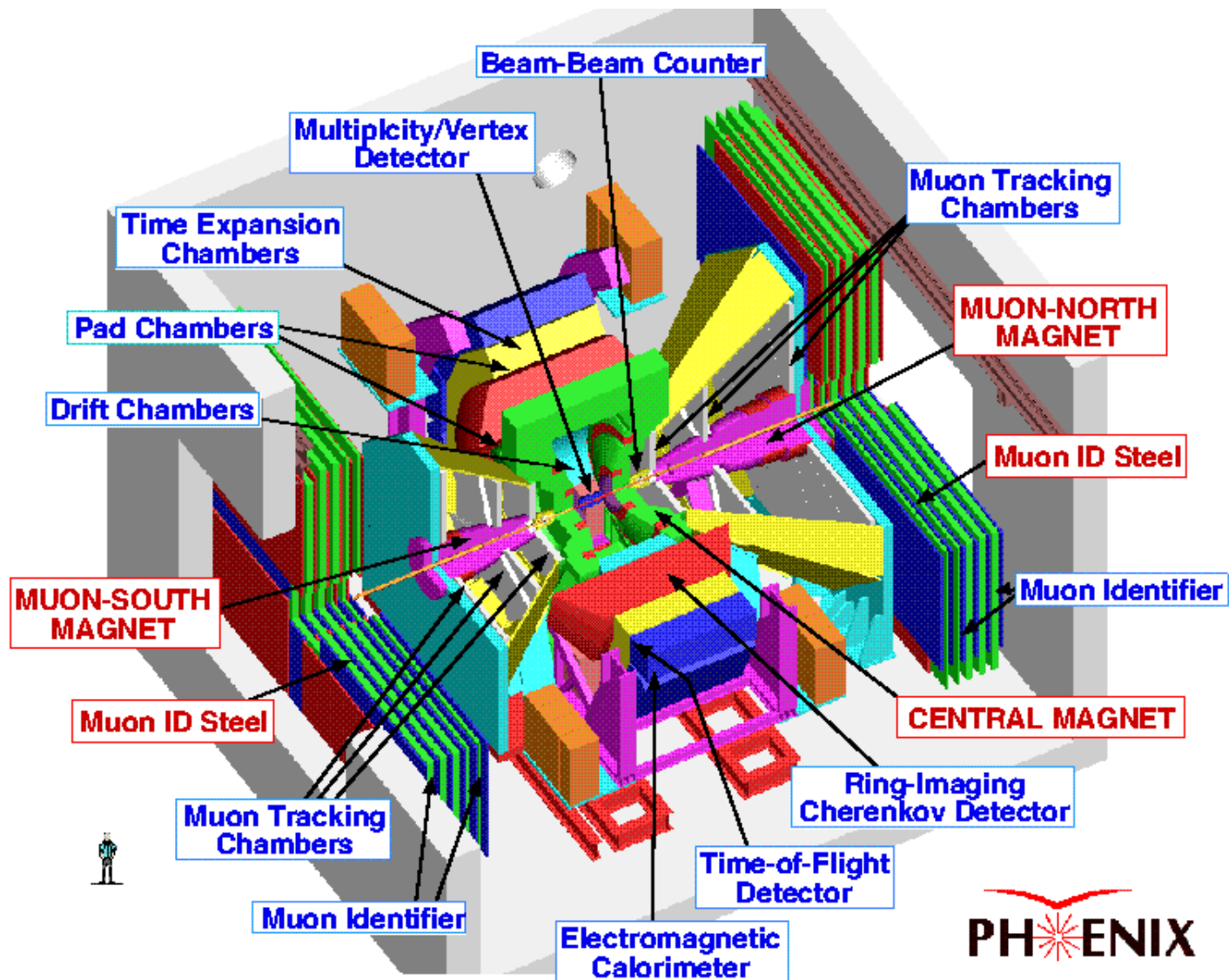


Figure 69: PHENIX detector at RHIC, dedicated to heavy ion collision studies

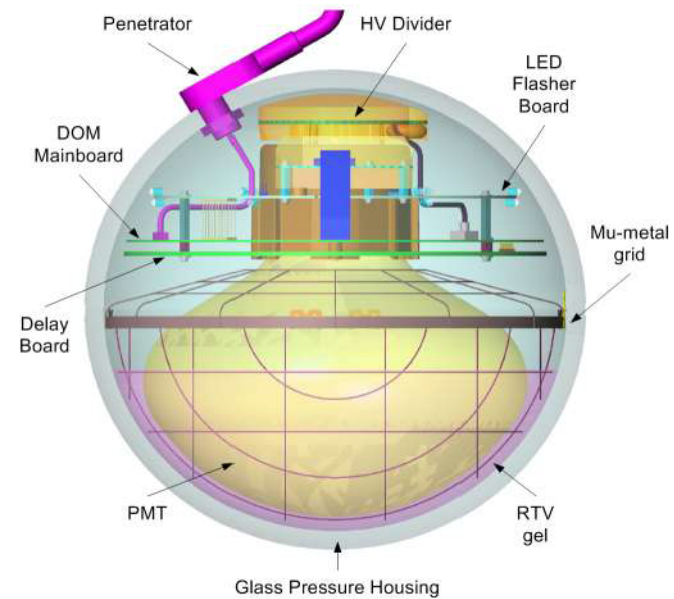
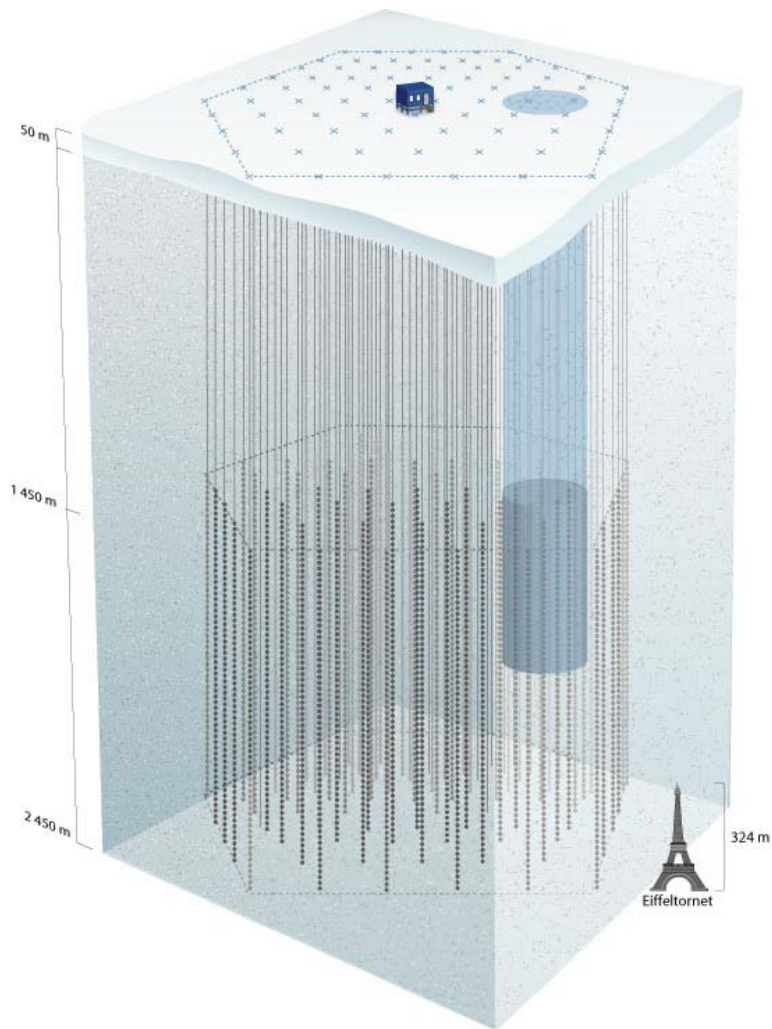


Figure 70: IceCube neutrino detector at the South Pole (left) is an array of photomultiplier modules (right)



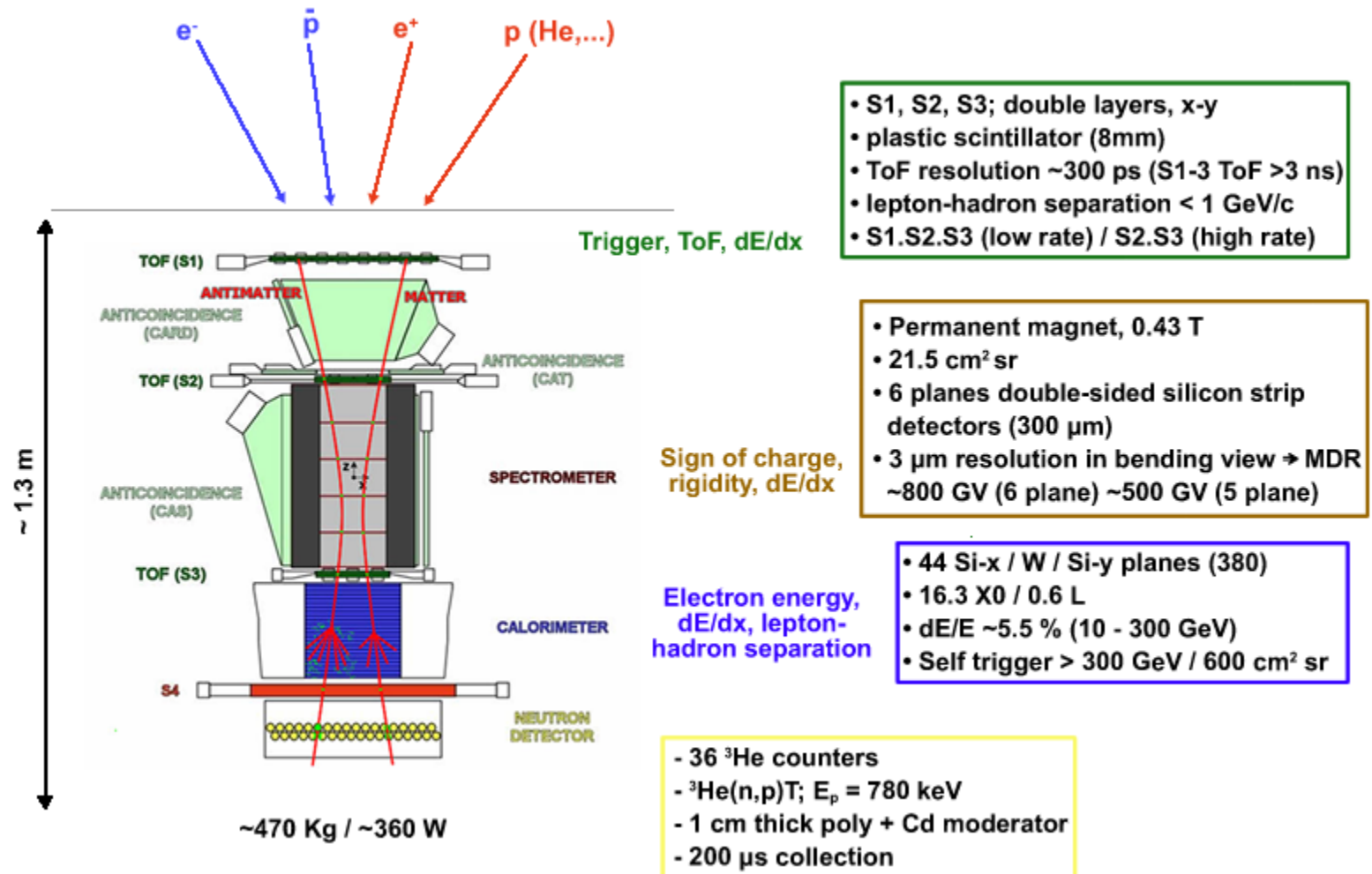


Figure 71: PAMELA detector in space, dedicated to antimatter and astrophysics studies